

## Determination of vortex the structure in

### $\kappa$ -(BEDT-TTF)<sub>2</sub>Cu(NCS)<sub>2</sub> by Josephson plasma resonance

M. M. Mola, S. Hill<sup>†</sup>, J. T. King and C. P. McRaven

*Department of Physics, Montana State University, Bozeman, MT 59717*

J. S. Qualls and J. S. Brooks

*Department of Physics and National High Magnetic Field Laboratory, Florida State University,*

*Tallahassee, FL 32310*

(May 19, 2019)

A cavity perturbation technique is used to study the microwave response of the organic superconductor  $\kappa$ -(BEDT-TTF)<sub>2</sub>Cu(NCS)<sub>2</sub>. Observation of a Josephson plasma resonance, below  $T_c$  ( $\sim 10$  K), enables investigation of the vortex structure within the mixed state of this highly anisotropic, type-II, superconductor. Contrary to previous assumptions, frequency dependent studies (28 – 153 GHz) indicate that a weak pinning theory previously derived by Bulaevskii *et al.* [Phys. Rev. Lett. **74**, 801 (1995)] most consistently describes our results. This weak pinning limit contrasts the behavior found in many layered oxide high- $T_c$  superconductors, as should be expected for these extremely clean molecular superconductors. Our data also suggests a transition in the vortex structure near the irreversibility line not previously observed in an organic superconductor using this technique.

PACS numbers: 71.18.+y, 71.27.+a, 74.25.Nf

It is widely acknowledged in the layered high- $T_c$  superconductors (HTSs) and, more recently, in the layered organic superconductors (OSs), that Josephson coupling is responsible for interlayer transport of superconducting pairs [1,2,3,4]. Magneto-optical experiments have been carried out by many groups, and for a wide range of materials, *e.g.* Bi<sub>2</sub>Sr<sub>2</sub>CaCu<sub>2</sub>O<sub>8+y</sub> (BSCCO) [1,2] YBa<sub>2</sub>Cu<sub>3</sub>O<sub>6-y</sub> (YBCO) [2], as well as several OSs [3,4]. These experiments

have demonstrated, in each case, that a Josephson plasma resonance (JPR) is observed in the inter-layer conductivity, and that this resonance may be used as an extremely sensitive tool for probing the vortex structure/dynamics.

$\kappa$ -(BEDT-TTF)<sub>2</sub>Cu(NCS)<sub>2</sub> (BEDT-TTF denotes bis-ethylenedithio-tetrathiafulvalene, or ET for short) is one in a series of highly anisotropic OSs, characterized by a layered structure. The conducting layers consist of a checkerboard pattern of face-to-face ET dimers, with nearest neighbor dimer pairs oriented perpendicularly [5]. These donor sheets exhibit near isotropic 2D conductivity within the **bc** plane. The insulating layers are formed from weakly bonded arrays of V-shaped Cu(NCS)<sub>2</sub> anions. The anisotropy parameter in the normal state, given by the ratio of the in-plane to out-of-plane conductivities  $\sigma_{bc}/\sigma_a$ , is  $\sim 1000$ . In the superconducting state, the anisotropy parameter is given by  $\gamma \equiv \lambda_{\perp}/\lambda_{\parallel} \sim 100 - 200$ , where  $\lambda_{\parallel}$  and  $\lambda_{\perp}$  are the London penetration depths for AC currents induced parallel ( $\lambda_{\parallel} \sim 0.8\mu m$ ) and perpendicular ( $\lambda_{\perp} \sim 100\mu m$ ) to the conducting layers respectively [6]. Such a large anisotropy makes this OS a prime candidate to study Josephson coupling, and changes in this coupling upon the introduction of supercurrent vortices into the sample, through the application of an external magnetic field.

In highly anisotropic superconductors, it is expected that the plasma mode for the low conductivity direction ( $\sigma_a$ ) lies below the superconducting gap *i.e.*  $\hbar\omega_p < 2\Delta$ . Below the critical temperature  $T_c$ , this plasma mode dominates the **a**-axis microwave response with frequency,  $\omega_p$ , which depends on the maximum inter-layer (or Josephson) current  $J_m(\mathbf{B}, T)$ , through the expression:

$$\omega_p(\mathbf{B}, T) = [8\pi^2 cs / \varepsilon_c \Phi_o] J_m(\mathbf{B}, T)$$

where

(1)

$$J_m = J_o \langle \langle \cos \varphi_{n,n+1}(\mathbf{r}) \rangle \rangle_t$$

$s$  is the crystal inter-layer spacing,  $\varepsilon_c$  is the high frequency permittivity,  $\Phi_o$  is the flux quantum,  $\varphi_{n,n+1}(\mathbf{r})$  is the gauge-invariant phase difference between layers  $n$  and  $n + 1$  at a

point  $\mathbf{r} = x, y$  in the  $\mathbf{bc}$  (high conductivity) plane, and  $\langle \dots \rangle_t$  and  $\langle \dots \rangle_d$  denote thermal and disorder averages.  $J_o(\mathbf{T}) = c\Phi_o/8\pi^2s\lambda_\perp^2(\mathbf{T})$  is the maximum inter-layer Josephson current density at zero field ( $B_{DC} = 0$ ), and  $\lambda_\perp$  is the inter-layer London penetration depth [7,8].

An important property of the Josephson coupling is the influence of an externally applied magnetic field on the collective plasma oscillation frequency  $\omega_p$ . When the applied DC field is parallel to the least conducting axis, a mixed state is created in which the field penetrates the sample in quantized flux tubes, generating supercurrent vortices in the superconductor.  $\varphi_{n,n+1}(\mathbf{r})$  depends explicitly on the vortex structure within this mixed state and is, thus, responsible for the field dependence of the resonance frequency  $\omega_p$  [7]. If the flux tubes form straight lines along the  $\mathbf{a}$ -axis,  $\langle \cos \varphi_{n,n+1}(\mathbf{r}) \rangle = 1$ , and maximum Josephson coupling occurs. However, in the presence of disorder, *e.g.* as a result of crystal defects which create vortex pinning sites, or through thermal fluctuations, the flux tubes will deviate from straight lines. This suppresses the maximum Josephson current. It is when AC currents are excited between the layers, at a frequency which corresponds to the natural frequency of the plasma oscillation ( $\omega_p$ ), that a sharp resonance is observed. Consequently, this resonance frequency provides a direct measurement of the maximum inter-layer current, which in turn can be used to probe vortex structure in the mixed state.

We have carried out experiments on several  $\kappa$ -(ET)<sub>2</sub>Cu(NCS)<sub>2</sub> single crystals. The dimensions of each crystal were approximately  $0.75 \times 0.5 \times 0.2$  mm<sup>3</sup>, with the low conductivity axis the shortest of the three. We found that all samples gave qualitatively similar results. Microwave transmission experiments were carried out using a cavity perturbation technique described elsewhere [9]. We used the TE01 $n$  modes of cylindrical copper cavities ( $n = 1, 2, 3, \text{etc.}$ ), and the TE112 mode of a rectangular copper cavity. The use of a range of cavities enabled wide frequency coverage from 28 – 153 GHz. Typical loaded Quality factors for these cavities for a given measurement were approximately  $5 \times 10^3$  to  $2.5 \times 10^4$ . The samples were placed in one of two configurations within the cavity, which correspond to two different microwave field configurations [9]. The first position induces strictly in-plane currents, with the AC microwave magnetic field perpendicular to the layers ( $H_{AC} \perp \mathbf{bc}$ ). The second

configuration, with  $H_{AC} \parallel \mathbf{bc}$ , generates both in-plane and inter-layer Josephson currents. Both cavity positions were such that the DC magnetic field ( $B_{DC}$ ) was perpendicular to the conducting planes, *i.e.*  $B_{DC} \parallel \mathbf{a}$ . Temperature control was achieved using a small resistive heater attached mechanically to the cavity, and a Cernox thermometer. DC magnetic fields were generated using an 8 T superconducting solenoid. Field sweeps were made from 0 – 8 T at a rate of approximately 1 T per minute.

Figure 1 shows dissipation due to in-plane currents, plotted versus magnetic field, for temperatures in the range 1.6 to 4.5 K; the frequency is 44.4 GHz and the traces are offset for clarity. As expected for this configuration, the dissipation ( $\propto$  surface resistance) increases monotonically with increasing DC field. Indeed, the surface resistance approximately follows a  $B_{DC}^{1/2}$  behavior, consistent with flux flow type dissipation [10]. Eventually, the entire crystal is driven normal ( $\mu_0 H_{c2} \sim 2 - 3$  T at 2 K), and the dissipation levels off. Hence, little field dependence is observed above  $H_{c2}$ . It is evident that this configuration shows no resonant behavior, and very little temperature dependence. These findings are in stark contrast to recent studies by Schrama *et al.* [11], where it is claimed that an observed resonance is attributable to the in-plane response.

In contrast, the second configuration ( $H_{AC} \parallel \mathbf{bc}$ ) gives very different results. Fig. 2 plots dissipation [ $\propto \sigma_a(\omega)$ ] versus magnetic field for several frequencies in the range 28 – 153 GHz; the temperature is 2.0 K in each case. A pronounced resonant feature can now be seen (indicated by arrows), which becomes sharper and moves to lower magnetic field upon increasing the frequency. Due to the absence of this resonance in the purely in-plane response (Fig. 1), we conclude that this behavior is related to the inter-layer coupling, and that insufficient care was taken to separate these contributions in the work of Schrama *et al.* [11,12]. The anti-cyclotron nature of the resonances shown in Fig. 2 has been well documented in the HTSs [13], and has also been observed in previous work on this OS [3], though only two frequencies were used. The wider frequency range employed here clearly confirms the anti-cyclotron trend.

Figures 3a and b show the temperature dependence of the field dependent dissipation for

$\omega_p/2\pi = 76$  and  $111$  GHz, respectively. Note that, as the temperature increases toward the superconducting to normal transition ( $T_c \sim 10$  K), the resonances vanish. This observation would seem to indicate that it is the superconducting carriers that are responsible for the sharp dissipative peak. This fact, along with the anti-cyclotronic nature of the resonance, and the AC current polarization dependence of the effect (*i.e.* resonances are not observed for  $H_{AC} \perp \mathbf{bc}$ ), leads us to conclude that the resonance indeed corresponds to a Josephson plasma mode. Note, no apparent hysteresis was observed for the up and down sweeps of the magnetic field in this material, hence only up sweeps are plotted for clarity.

Looking more closely at the  $76$  GHz data in Fig. 3a, we see that the resonance peak position decreases monotonically with respect to increasing temperature. This behavior is consistent with previous observations in this OS [3], however, we see an entirely different temperature dependence in the tail of the resonance. The structure in the low field tail ( $\sim 0.1$  T) shows an initial increase in field with increasing temperature, reaching a maximum, then decreasing back to zero field as  $T_c$  is approached. This so-called "cusp" behavior has been observed in some HTSs [13], but never in any of the OSs.

For the  $111$  GHz data in Fig. 3b, we see a similar resonance structure, but now the cusp behavior can be seen in the position of the resonance rather than its tail. The phenomenon responsible for the cusp has not changed, however, the JPR has been pushed to lower field by working at higher frequencies, thereby moving the resonance position into the cusp regime.

Measurements spanning a broad frequency range, as shown in Fig. 4, indicate that the cusp behavior is confined to a relatively narrow field and temperature domain. In fact, comparison of the cusp position with published magnetization data [14,15] show that it falls along, or very near to, the irreversibility line. Due to the change in nature of the temperature dependence of the JPR at the cusp position, we conclude that there is a transformation in the vortex structure at (or near) the irreversibility line.

It is well known that a dimensional crossover phenomenon, between a three-dimensional flux-line-lattice and a two-dimensional pancake structure, occurs at approximately  $10$  mT in  $\kappa-(\text{ET})_2\text{Cu}(\text{NCS})_2$  [16,17]. Thus, it is assumed that, over a large portion of the super-

conducting phase diagram probed in this work (and shown in Fig. 4), the vortex structures in adjacent layers are completely decoupled. We propose that the cusp phenomenon is associated with a quasi-two-dimensional (Q2D) vortex lattice to vortex liquid transition [18,19].

Intra-layer vortex-vortex interactions are expected to create an ordered array (Q2D solid) of pancake vortices in each layer. Random defects will tend to pin each Q2D solid in such a way that there is little correlation between the locations of the vortices in each layer, *i.e.*  $\langle \cos \varphi_{n,n+1} \rangle$  will be small, and inter-layer Josephson tunneling will be suppressed. Upon increasing the temperature, thermal fluctuations will tend to cause the vortices in each layer to deviate from their mean positions. Provided that these displacements are small compared to the distance between adjacent vortices, the effect of increasing temperature will actually result in an increase in the tunneling probability and, hence, an increase in the maximum inter-layer Josephson current.

2D melting occurs when the thermal (or quantum) fluctuations in the locations of the vortices are on the order of the inter-vortex separation, *i.e.* either when the flux density exceeds a critical value  $\mathbf{B}_m(T)$ , or when the temperature exceeds a critical value  $T_m(\mathbf{B})$ . In the liquid phase, when there exists no ordered vortex state, increased thermal fluctuations (*i.e.* increasing temperature) will tend to suppress inter-layer tunneling and, hence, the maximum inter-layer Josephson current. Thus, entirely opposite temperature dependences of the JPR frequency are expected in the Q2D solid and liquid phases (see Eq. 1).

We can now relate the observed field and temperature dependence of the resonances to the above discussion. Application of a magnetic field tends to reduce the resonance frequency (see discussion below). Thus, for a fixed frequency measurement, a resonance is observed when the field dependent plasma frequency  $\omega_p(\mathbf{B},T)$  matches the measurement frequency. Consequently, any trend that increases  $\omega_p(\mathbf{B},T)$  will shift the observed resonance to higher magnetic fields, since a stronger field is required to reduce  $\omega_p(\mathbf{B},T)$  so that it matches the measurement frequency. The converse is true for trends which decrease  $\omega_p(\mathbf{B},T)$ . Thus, in the Q2D solid phase, increasing temperature will tend to shift the resonance to higher field while, in the liquid phase, one expects the resonance to move to lower fields upon increasing

the temperature. This is precisely the behavior observed in Fig. 4b, where the cusp marks the change in temperature dependence and, therefore, the transition between Q2D solid and liquid phases. Although the dashed line in Fig. 4b marks the irreversibility line, it is believed that the melting curve lies close to this line.

Finally, we consider the frequency dependence of the resonance (at constant temperature). It has been previously assumed for this substance that the frequency of the resonance ( $\omega_p$ ) obeys a power law field dependence of the form

$$\omega_p^2 = A\mathbf{B}^{-\mu} \exp(T/T_c), \quad (2)$$

where A is a constant. The inset to Fig. 5 shows the best fit to a powerlaw, for T = 2.0 K. From such a fit we obtain a value for the exponent of  $\mu = 0.7$ , consistent with previous work, where only two data points were available [3]. However, this is clearly not a good fit when data spanning a wider range of frequencies is available. In the main panel of Fig. 5, we show a fit to the weak pinning theory of Bulaevskii *et al.* [7], where a decaying exponential field dependence of  $\omega_p(\mathbf{B}, T)$  is predicted. In this case,

$$\omega_p^2 = (8\pi^2/\varepsilon_c\Phi_o) \exp[-(B/B_D)^{3/2}]$$

where (3)

$$B_D = [\Phi_o^{11/3}/(4\pi)^3] (2\pi\gamma_o E_p)^{3/2} s^2 \lambda_{\parallel}^4.$$

$B_D$  is a de-coupling field, above which, phase coherence between the layers is lost;  $\gamma_o$  is the anisotropy parameter;  $E_p$  is a pinning parameter; and  $\lambda_{\parallel}$  is the in-plane penetration depth [8]. Clearly, this expression gives a much better fit, from which we are able to extract various sample parameters. Using  $\varepsilon_c = 25$ ,  $\gamma_o = 100-200$ , and  $\lambda_{\parallel} = 1 \mu\text{m}$  [6], we find the zero field maximum interlayer current density,  $J_o = 2 \times 10^3 \text{ A cm}^{-2}$ . From this, we are able to deduce the interlayer penetration depth,  $\lambda_{\perp} = 90 \mu\text{m}$ , which is on the order of previous measurements [6]. Further, we find a value for the decoupling field,  $B_D = 0.7 \text{ T}$ , from which

we can extract the pinning parameter  $E_p = 6.3 \times 10^{-13}$  to  $1.3 \times 10^{-12}$   $\text{J}^2\text{m}^{-4}$ . This range of values is three orders of magnitude lower than the BSCCO measurements discussed in ref. [20]. This is not surprising, since it is well established that the ET salts are considerably cleaner systems than the HTSs, thus having far fewer pinning sites. Moreover, for the weak pinning limit, it has been noted that the in-plane critical current depends on the pinning parameter given above [20]:

$$J_{ab} = (4c/3\Phi_o)(E_p/3)^{1/2}. \quad (4)$$

Using the range of values above for  $E_p$ , we find the critical in-plane current to be in the range,  $J_{ab} = 3 \times 10^4$   $\text{A cm}^{-2}$  to  $4 \times 10^4$   $\text{A cm}^{-2}$ , consistent with values obtain by other methods [3]. Thus our measurements have proven consistent with previous work, and seem to agree excellently with the weak pinning theory of Bulaevskii *et al.* [7]. It should be noted, however, that we see a slight sample dependence in our measurements, as well as some variance compared to other published data [3,11]. This sample dependence is not surprising given the dependence of  $\omega_p(\mathbf{B},T)$  on the pinning parameter  $E_p$ , which is liable to depend on sample quality. Thus, we should expect small deviations from the numbers given above, for different samples of  $\kappa-(\text{ET})_2\text{Cu}(\text{NCS})_2$ .

In conclusion, Josephson plasma resonance measurements have provided a wealth of information about the organic charge transfer salt  $\kappa-(\text{ET})_2\text{Cu}(\text{NCS})_2$ . In particular, this has proven to be a useful method of probing both the inter-layer as well as the in-plane characteristics of this superconductor. The extremely clean (at least three orders of magnitude cleaner than the HTSCs) nature of this material necessitates use of the weak pinning theory of Bulaevskii *et al.* to analyze our data. From this model, we are able to extract various material parameters, *e.g.* the inter-layer penetration depth, the decoupling field, the pinning parameter, and the in-plane critical current. This novel technique has also allowed us to investigate the Q2D vortex structure; we see an apparent Q2D solid to liquid transition, leading to a cusp in the temperature dependence of the plasma frequency  $\omega_p(\mathbf{B},T)$ . Further

examination of the cusp, and the behavior at the irreversibility line should lead to a better understanding of the observed transition.

This work was supported by the Petroleum Research Fund (33727-G3) and the Office of Naval Research (N00014-98-1-0538). CPM and JTK acknowledge support through the NSF REU program (nsf-dmr 9820388).

---

<sup>†</sup> email: hill@physics.montana.edu

- [1] Y. Matsuda, M. B. Gaifullin, K. Kumagai, K. Kadowaki, and Y. Mochiku, *Phys. Rev. Lett.* **75**, 4512 (1995).
- [2] H. Shibata and T. Yamada, *Phys. Rev. B* **54**, 7500 (1996).
- [3] T. Shibauchi, M. Sato, A. Mashio, T. Tamegai, H. Mori, S. Tajima, and S. Tanaka, *Phys. Rev. B* **55**, R11 977 (1997).
- [4] T. Shibauchi, M. Sato, S. Ooi, and T. Tamegai, *Phys. Rev. B* **57**, R5622 (1998).
- [5] T. Ishiguro, K. Yamaji, and G. Saito, *Organic Superconductors* (Springer-Verlag, Berlin, 1998).
- [6] P.A. Mansky, P.M. Chaikin, and R.C. Haddon, *Phys. Rev. B* **50**, 15929 (1994).
- [7] L. N. Bulaevskii, M. P. Maley, and M. Tachiki, *Phys. Rev. Lett.* **74**, 801 (1995).
- [8] L.N. Bulaevskii, V.L. Pokrovsky, and M.P. Maley, *Phys. Rev. Lett.* **76**, 1719 (1996).
- [9] M. Mola, S. Hill, M. Gross, and P. Goy, *Rev. Sci. Inst.* **71**, 186 (2000), and references therein; also cond-mat/9907310.
- [10] M.W. Coffey and J.R. Clem, *Phys. Rev. Lett.* **67**, 386 (1991).
- [11] J. M. Schrama, E. Rzepniewski, R. S. Edwards, J. Singleton, A. Ardavan, M. Kurmoo, and P. Day, *Phys. Rev. Lett.* **83**, 3041 (1999).

- [12] S. Hill, M. Mola, N. Harrison, and J. Wosnitzer, submitted to Phys. Rev. Lett.
- [13] O.K.C. Tsui, N. P. Ong, Y. Matsuda, Y. F. Yan, and J. B. Peterson, Phys. Rev. Lett. **73**, 724 (1994).
- [14] M. Lang, F. Steglich, N. Toyota, and T. Sasaki, Phys. Rev. B **49**, 15227 (1994).
- [15] T. Sasaki, W. Biberacher, K. Neumaier, W. Hehn, K. Andres, and T. Fukase, Phys. Rev. B **57**, 10889 (1998).
- [16] T. Nishizaki, T. Sasaki, T. Fukase, and N. Kobayashi, Phys. Rev. B **54**, R3760 (1996).
- [17] S. J. Blundell, S.L. Lee, F. L. Pratt, C. M. Aegerter, Th. Jestadt, B. W. Lovett, C. Ager, T. Sasaki, V. N. Laukhin, E. Laukhina, E. M. Forgan, and W. Hayes, Synth. Met. **103**, 1925 (1999); and references therein.
- [18] A. Houghton, R.A. Pelcovits, and A. Sudbø, Phys. Rev. B **40**, 6763 (1989).
- [19] L. Fruchter, A. Aburto, and C. Pham-Phu, Phys. Rev. B **56**, 2936 (1997).
- [20] C.J. van der Beek, P. H. Kes, M. P. Maley, M. J. V. Menken, and A. A. Menovsky, Physica C **195**, 307 (1992).

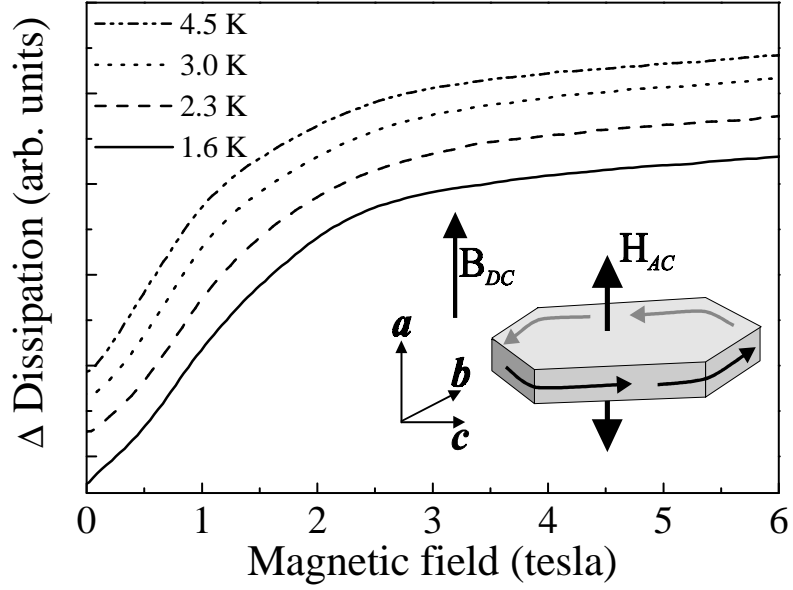


FIG. 1. Field dependent dissipation ( $\propto$  surface resistance) due to in-plane currents, at various temperatures, and for  $\omega/2\pi = 44.4$  GHz (offset for clarity). As expected for flux flow type dissipation, the surface resistance varies approximately as  $B^{1/2}$  for  $B < \mu_0 H_{c2}$ . This configuration shows no resonant behavior and little temperature dependence.

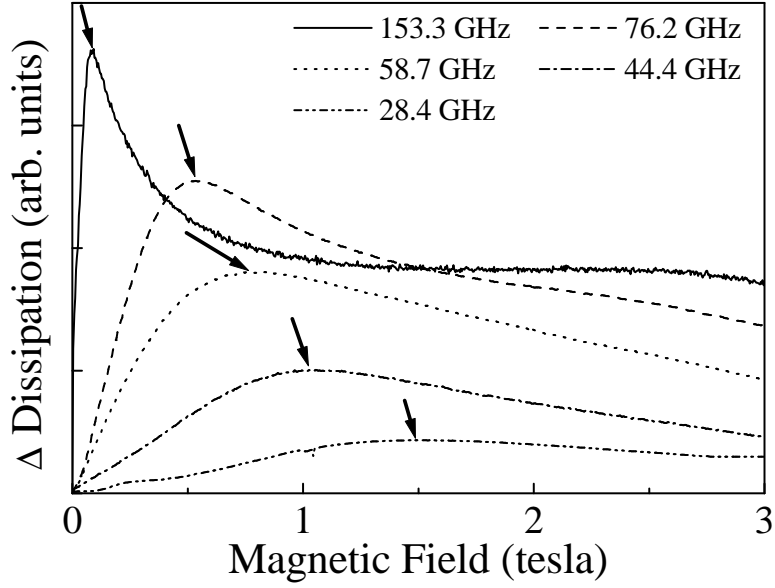


FIG. 2. Magnetic field sweeps, at various frequencies, with  $H_{AC} \parallel \mathbf{bc}$ ; the temperature is 2.0 K in each case. Notice the sharp resonance feature, indicated by arrows, which is attributable to inter-layer Josephson currents. Note that the resonance field position,  $B_o$ , decreases with an increasing frequency, *i.e.* anti-cyclotron behavior.

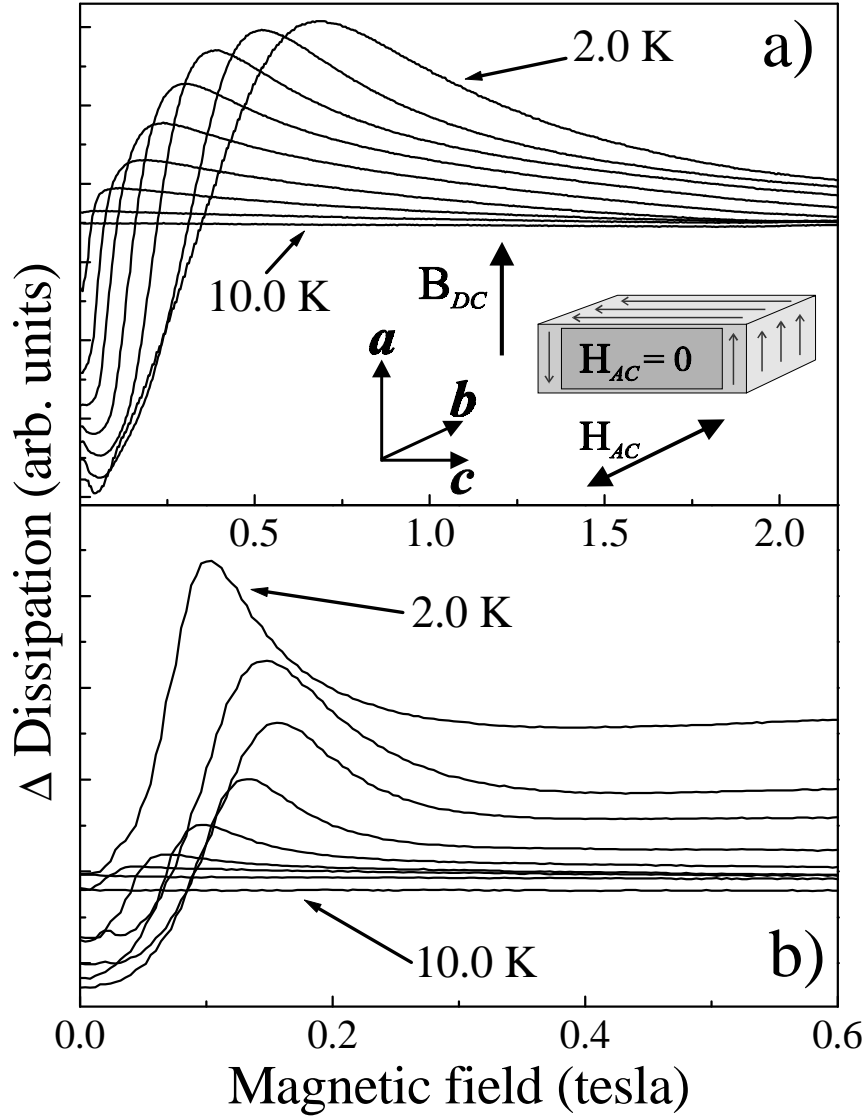


FIG. 3. Temperature dependence of the Josephson plasma mode for a)  $\omega/2\pi = 76$  GHz and b)  $\omega/2\pi = 111$  GHz. Notice that in a), the resonance peak position decreases monotonically as a function of temperature; however, the structure in the tail of this resonance exhibits a "cusp" behavior. In contrast, due to the anti-cyclotronic behavior of the JPR, the resonance in b) has moved to lower field, and we now see a cusp behavior in the resonance position.

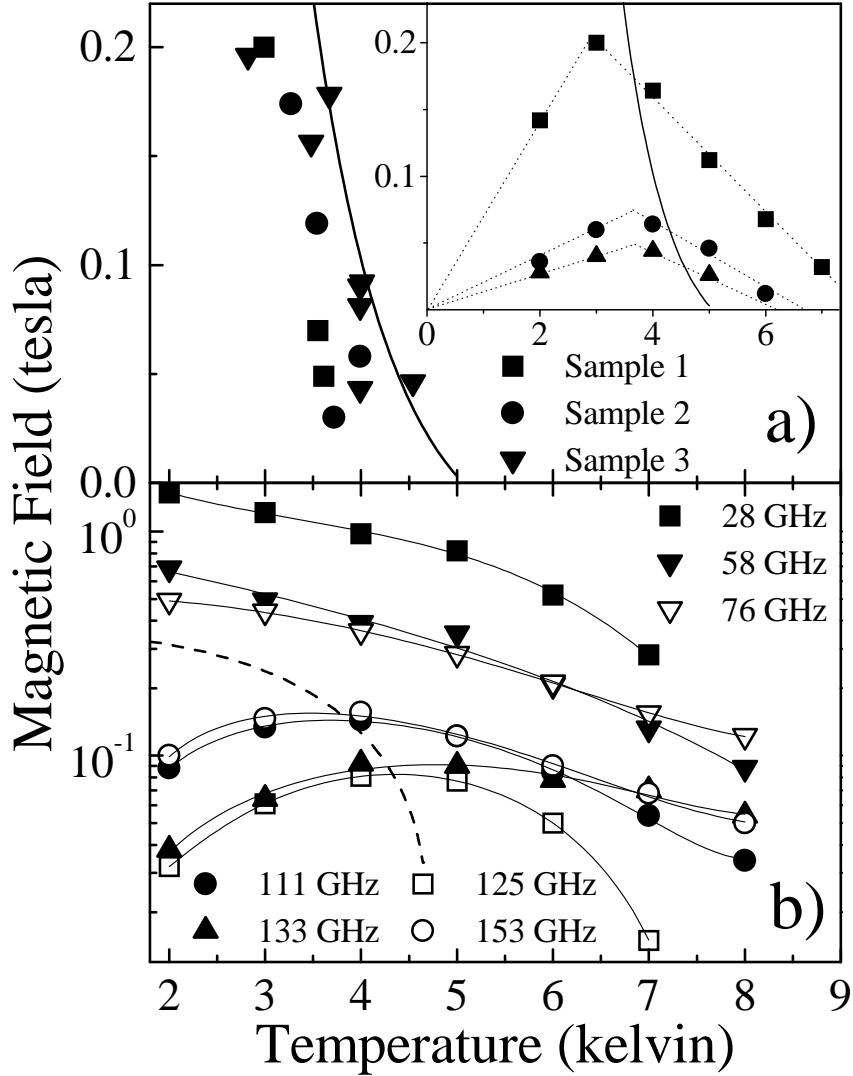


FIG. 4. a) Plot of the cusp positions in field, versus temperature, for several samples and frequencies; the inset plots several representative series of resonance fields (for a single sample and a range of frequencies) versus temperature, and the method used to determine the location of the cusp, *i.e.* the crossing points of the extrapolated fits (dashed lines) to the low and high temperature behavior. The cusp positions in the main panel of a) are scattered around the irreversibility line (solid line). b) Resonance field  $B_0$  vs. temperature for measurements spanning a wide frequency range (28-153 GHz), and for several samples. The higher frequencies exhibit a cusp behavior, while lower frequencies show a monotonic temperature dependence. The dashed line indicates approximate position of irreversibility line, and the solid lines are guides to the eye.

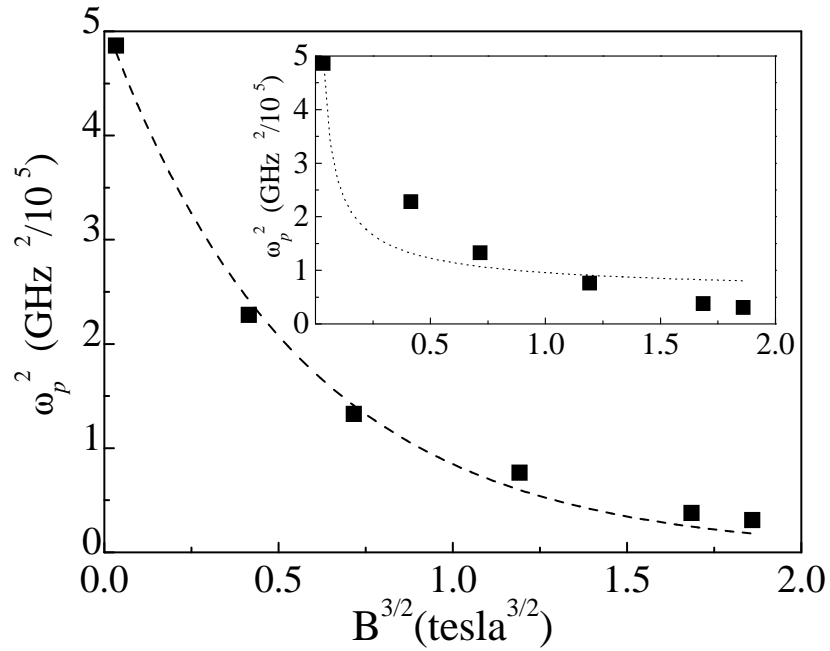


FIG. 5. When  $\omega_p^2$  is plotted against  $B^{3/2}$ , we see an exponential decay. This behavior is expected for the weak pinning limit. This analysis gives a value of  $B_D$  for this material of  $\sim 0.7$  T. Inset: we have tried to fit the data with a powerlaw, as has been observed in the HTSs, and previously claimed in this material [3]. However, this is clearly not a good fit when a wider frequency interval is sampled.